Quasiresonant exciton spin orientation and alignment in a single quantum dot under zero and nonzero magnetic fields

R. Kaji,* S. Adachi, T. Shindo, and S. Muto
Department of Applied Physics, Hokkaido University, N13 W8, Kitaku, Sapporo 060-8628, Japan
(Received 1 September 2009; revised manuscript received 18 November 2009; published 29 December 2009)

The polarization conversion from optical orientation to alignment in single InAlAs/AlGaAs quantum dots (QDs) was studied in detail under zero and nonzero magnetic fields. Under the influence of the effective magnetic field, bright exciton doublets precess in pseudospin space, where the torque vector is composed of the external magnetic field and the anisotropic exchange field. For a number of QDs, we measured the angle difference of the polarization axes obtained with circularly polarized excitations, which is an indicator of the conversion efficiency under a zero magnetic field. By applying a longitudinal magnetic field, a high conversion efficiency of ~50% was achieved. Additionally, the exciton spin-relaxation time and the magnitude of built-in linear dichroism were estimated from the exciton spin dynamics using the three-dimensional pseudospin precession model, and a long spin-relaxation time exceeding the recombination lifetime was obtained. Finally, we discussed the influence of a nuclear magnetic field on the polarization conversion.

DOI: 10.1103/PhysRevB.80.235334 PACS number(s): 78.67.Hc, 72.25.Fe, 71.35.Ji, 78.55.Cr

I. INTRODUCTION

Studies on dynamics of localized spins in semiconductor quantum dots (QDs) have attracted considerable attention from both fundamental and practical points of view. For the application of these QDs to quantum information processing[1] and to develop QD lasers and single-photon sources, it is very important to study the polarization of the emitted photons associated with exciton annihilation. For ideal QDs, the relevant eigenstates are bright excitons formed by circularly polarized photons with the angular momentum of ± 1, and the emission is found to be circularly polarized (σ_+ or σ_-) via the selection rule of optical transitions. However, actual QDs have an anisotropic shape and strain distribution originating from the QD formation process, and as a result, the confinement potential symmetry is reduced from D_{2d} to C_{2v} or lower.[2] Since the anisotropic exchange interaction (AEI) caused by the symmetry reduction works as an in-plane magnetic field effectively, the precession of exciton spin with frequency $\Omega_{\mathrm{exc}}(=\delta_{\mathrm{b}}/\hbar)$ can occur even under a zero external magnetic field. Here, δ_{b} denotes the exciton fine-structure splitting (FSS) and is on the order of several tens microelectron volts for typical self-assembled InAlAs QDs. Consequently, the AEI modifies the bright exciton eigenstates from $|\pm 1\rangle$ to $|+1\rangle \pm |-1\rangle$, and at the recombination lifetime, a part of polarization becomes linear (x or y). Since an exciton created with circularly polarized photon tends to emit linearly polarized photon, this phenomenon can be interpreted as "polarization conversion." Several studies on phenomena related to similar conversion in QD ensembles have already been reported [for example, InAlAs/AlGaAs QDs (Ref. 3) and CdSe/ZnSe QDs (Ref. 4)]. However, it is difficult to determine the intrinsic parameters from the ensemble average over QDs having inhomogeneous shape and strain distribution.

In this study, we study the polarization conversion for single InAlAs/AlGaAs QDs. The quasiresonant excitation results in high conversion efficiency under zero and nonzero longitudinal magnetic fields. Considering the exciton spin dynamics based on a precessional decoherence model enables us to estimate the exciton spin-relaxation time and the magnitude of built-in linear dichroism. Additionally, we discuss the influence of optically created nuclear field on the polarization conversion.

II. EXPERIMENTS

We used self-assembled $In_{0.75}Al_{0.25}As/Al_{0.3}Ga_{0.7}As$ QDs that were grown on a (100) GaAs substrate by molecular-beam epitaxy.[5] Atomic force microscopy measurements on a reference sample, i.e., an uncapped QDs with the same growth conditions, revealed that the average height and diameter of QDs are ~4 and ~20 nm, respectively, with the QD density of ~500 μm^{-2}. To perform single QD spectroscopy, small mesa structures with a typical diameter of ~150 nm were fabricated by wet etching and electron-beam lithography.

A cw Ti:sapphire laser was used to excite the QD sample at 745 nm (~1.664 eV). As shown later, this photon energy corresponds to the quasiresonant excitation of a target InAlAs QD. The photoluminescence (PL) signals were collected by using an objective lens and detected with a 0.64 m triple grating spectrometer and a liquid nitrogen cooled Si charge-coupled device array. The typical accumulation time with a high signal to noise ratio is 2 s. Though the energy resolution of our setup is ~12 μeV, it can be improved to 5 μeV by spectral fitting. The sample temperature was maintained at ~5 K, and a magnetic field up to 5 T was applied in the Faraday geometry ($\boldsymbol{B} \| \boldsymbol{k}$). The excitation polarization was fixed to be circularly polarized (σ_+ or σ_-) by using a quarter-wave plate, and the polarization of PL spectra was analyzed with a half-wave plate (HWP) and a polarizer introduced in the detection path before the spectrometer.

III. RESULTS AND DISCUSSION

A. Without magnetic field

To study the polarization conversion from optical orientation to alignment, bright excitons have to be efficiently gen-

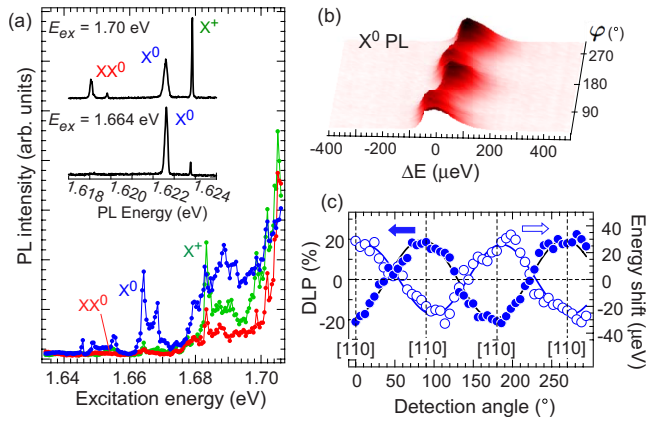

FIG. 1. (Color online) (a) PL excitation spectra measured at PL energy of X^0, X^+, and XX^0. At the energy of 1.664 eV (~43 meV above the X^0 ground state), X^0 PL is observed dominantly. Insets: PL spectra of target single QD with wetting layer excitation (upper inset) and with quasiresonant excitation (lower inset). (b) Three-dimensional plot of X^0 PL intensity. The energy and intensity changes due to AEI are clearly measured. (c) Energy shift (open circles) and DLP (closed circles) under circularly polarized excitation. In both figures, the detection angle φ was used as a function.

erated and injected into their ground states. For this purpose, the excitation energy was tuned to 1LO resonance of the exciton ground state. It is well known that in InAlAs/AlGaAs QDs,[3] CdSe/ZnSe QDs,[4] and InAs/GaAs QDs,[6] LO phonon-assisted excitation causes the fast energy relaxation of photogenerated excitons, preserving the degree of spin polarization. Correspondingly, this excitation energy can be used for effective injection of excitons with high spin polarization.

Figure 1(a) shows the time-integrated PL spectra measured at the PL energy of a neutral exciton (X^0), a neutral biexciton (XX^0), and a positively charged exciton (X^+) by varying the excitation energy (E_{ex}) under a zero magnetic field. Their charge states are assigned using a variety of methods, e.g., from the FSS measurements,[7] the autocorrelation of PL,[8] and binding energy.[9] In the case of the wetting layer excitation ($E_{ex} \sim 1.70$ eV), as shown in the upper inset, the emissions from not only X^0 but also XX^0 and X^+ are observed simultaneously, and their intensity decreases gradually with E_{ex} reflecting the reduced density of states. At $E_{ex} = 1.664$ eV, X^0 shows an abrupt increase (lower inset), which is identified as LO phonon-assisted excitation. All the experimental data shown hereafter were obtained at this excitation energy.

When the polarization of X^0 emissions was analyzed with a rotating HWP and a polarizer, not only PL energy [Fig. 1(c), open circles] but also intensity [Fig. 1(b)] showed periodical changes under circularly quasiresonant excitation. In these analyses, the detection angle φ was varied. The peak-to-peak amplitude of the energy shift of ~50 μeV corresponds to the FSS (δ_b), and the intensity modulation indicates the occurrence of the circular to linear (C→L) polarization conversion. In this study, the degree of linear polarization (DLP) is used as a key index of the conversion efficiency and is defined as $\rho = (I_\varphi - I_{\varphi+\pi/2})/(I_\varphi + I_{\varphi+\pi/2})$. Here,

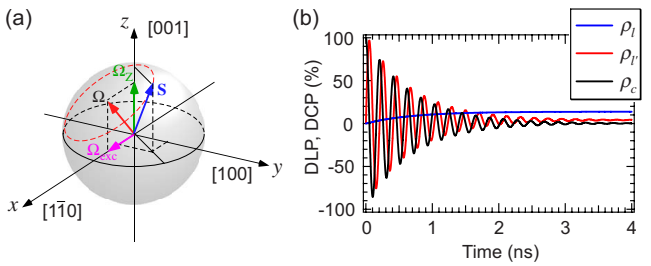

FIG. 2. (Color online) (a) Sketch of spin $\boldsymbol{S}$ and torque vector $\boldsymbol{\Omega}$ in the Bloch sphere under a longitudinal magnetic field. Here, Ω_Z is a component of the torque induced by the external magnetic field, and Ω_{exc} is that induced by the anisotropic exchange field. (b) Example of time evolution of DLP and DCP under a zero external field. In this case, $\rho_{l'}$ and ρ_c are components perpendicular to $\boldsymbol{\Omega}$. It is found that the oscillations of $\rho_{l'}$ and ρ_c decay and ρ_l converges to Y_l. The DLP and DCP are determined by the balance between the coherent precession and spin decay time.

$I_\varphi(I_{\varphi+\pi/2})$ is the PL intensity in the $\varphi(\varphi+\pi/2)$ frame. As shown in Fig. 1(c), the DLP is about 20% for X^0 PL under a zero magnetic field. More detailed discussion about this large DLP will be presented in the next section.

B. Model calculation

For a more detailed analysis, we introduce exciton pseudospin. If we treat the bright exciton doublet $|\pm 1\rangle$ as an effective pseudospin with $\boldsymbol{S} = \pm 1/2$, the exciton spin state can be depicted as a vector $\boldsymbol{S}$ in the Bloch sphere [Fig. 2(a)]. We also consider the mutual conversion between $\boldsymbol{S}$ and $\boldsymbol{\rho}$, where $\boldsymbol{\rho}$ is a vector in the Poincare sphere indicating light polarization. In this case, the dynamics of the exciton spin ("pseudospin" to be more precise) is described by the following rate equation:[4,10]

$$\frac{\partial \boldsymbol{S}}{\partial t} = \boldsymbol{\Omega} \times \boldsymbol{S} - \frac{1}{\tau_s}(\boldsymbol{S} - \boldsymbol{P}_{eq}) - \frac{1}{\tau_R}(\boldsymbol{S} - \boldsymbol{P}_{ex}), \qquad (1)$$

where τ_s and τ_R are the exciton decay time due to spin relaxation and recombination, respectively. The vector $\boldsymbol{P}_{ex} = (P_l, P_{l'}, P_c)$ is the excitation polarization vector in the Poincare sphere and is also considered as the initial spin state in the Bloch sphere. Here, P_l and $P_{l'}$ are the DLP along the $[1\bar{1}0]$ and $[100]$ crystallographic axes, respectively, and P_c is the degree of circular polarization (DCP: projection on $[001]$). The first term on the rhs of Eq. (1) represents the coherent spin precession induced by the effective field $\boldsymbol{\Omega}$, and the second (third) term represents the decay of the spin vector due to exciton spin relaxation (recombination). Under a zero external magnetic field, the torque vector $\boldsymbol{\Omega}$ can be written as $\boldsymbol{\Omega} = (\Omega_{exc}, 0, 0)$ and lies in the equatorial plane of the sphere. When an exciton is recombined, the information of $\boldsymbol{S}$ is transferred to $\boldsymbol{\rho}$, which determines the polarization of emission. By using the Stokes parameters ρ_l, $\rho_{l'}$, and ρ_c, which describe the DLP along $[1\bar{1}0]$, $[100]$, and the DCP, $\boldsymbol{\rho}$ can be written as $\boldsymbol{\rho} = (\rho_l, \rho_{l'}, \rho_c)$, where $|\boldsymbol{\rho}| = \sqrt{\rho_l^2 + \rho_{l'}^2 + \rho_c^2} \leq 1$.

It is worth noting that the dynamics model includes the polarization equilibrium $\boldsymbol{P}_{eq} = (Y_l, 0, 0)$, where Y_l originates

from the built-in linear dichroism of a QD. Y_l gives the convergence direction and brings the attracting force into the xy plane, thereby affecting $\boldsymbol{S}$. As is well known, the valence-band mixing (VBM) due to the anisotropy of the strain distribution modifies the bright exciton eigenstates, and consequently induces the strong linear polarization.[11] If the anisotropy of the strain distribution, not the asymmetry of the QD shape, influences Y_l crucially, $\boldsymbol{P}_{\mathrm{eq}}$ may not be positioned along the Ω_{exc} direction, because the major axis of the strain distribution shifts from the direction of the exchange field in single CdTe/ZnTe QDs.[12] Although, in our InAlAs QD the impact of VBM is less significant compared with these II-VI QD samples, the effect of VBM should contribute to the built-in linear dichroism. Since the parameter Y_l can include the effect of VBM, thermalization, and other unknown factors, the introduction of Y_l gives a flexible treatment of the results. In order to identify the major origin of Y_l, other independent experiments are necessary. For simplicity, we assume that Y_l has the same sign as Ω_{exc}, and $\boldsymbol{P}_{\mathrm{eq}}$ is in the $[1\bar{1}0]$ axis, as assumed most commonly in many studies.

Figure 2(b) shows an example of the time evolution of the polarization with σ_+ excitation under a zero external magnetic field. $\rho_{l'}$ and ρ_c, which are perpendicular to the torque vector, oscillate with the frequency Ω_{exc} and decay to zero within a typical time interval. Meanwhile, ρ_l shows a monotonic increase and approaches the value of Y_l. From Eq. (1), steady-state polarizations can be given as follows:

$$\rho_l = \left(\frac{Y_l}{\tau_{\mathrm{s}}} + \frac{P_l}{\tau_{\mathrm{R}}}\right) T_{\mathrm{s}}, \tag{2}$$

$$\rho_{l'} = \frac{T_{\mathrm{s}}}{\tau_{\mathrm{R}}}\left[\frac{P_{l'}}{1+(\Omega_{\mathrm{exc}}T_{\mathrm{s}})^2} - \frac{\Omega_{\mathrm{exc}}T_{\mathrm{s}}P_c}{1+(\Omega_{\mathrm{exc}}T_{\mathrm{s}})^2}\right], \tag{3}$$

$$\rho_c = \frac{T_{\mathrm{s}}}{\tau_{\mathrm{R}}}\left[\frac{P_c}{1+(\Omega_{\mathrm{exc}}T_{\mathrm{s}})^2} + \frac{\Omega_{\mathrm{exc}}T_{\mathrm{s}}P_{l'}}{1+(\Omega_{\mathrm{exc}}T_{\mathrm{s}})^2}\right]. \tag{4}$$

Here, T_{s} is the exciton spin lifetime and is given by $T_{\mathrm{s}} = (\tau_{\mathrm{R}}^{-1} + \tau_{\mathrm{s}}^{-1})^{-1}$. Using Eqs. (3) and (4) the conversion from circular to linear polarization ($P_c \rightarrow \rho_{l'}$) and vice versa ($P_{l'} \rightarrow \rho_c$) can be predicted. Further, it should be noted that the observed DLP in the following measurements can be written as $\rho(\varphi) = \rho_l \cos(\varphi) + \rho_{l'} \sin(\varphi)$ in the laboratory frame.

Hanle effect, which is a depolarization due to an in-plane external magnetic field, is one of the results obtained by this precessional decoherence model and is depicted as Eq. (4) with $P_{l'}=0$ and $\Omega_{\mathrm{exc}}=\Omega_{\mathrm{x}}$. Here, Ω_{x} is the precession frequency induced by the in-plane magnetic field. Hanle measurement is one of the powerful methods to evaluate the spin lifetime of the associated carrier spins, and so far has been used for a several QD samples.[13–15] Since these works treated with some kinds of the carrier spins (e.g., an electron spin, an exciton pseudospin, and a hole spin), discussion about the spin dynamics would be more complicated. But underlying physics is quite similar, and the T_{s} obtained in this study can be compared directly with the results of Hanle measurements. The understanding of the spin dynamics is essential to the control of the spin precession which allows to optimize the polarization conversion degree, and therefore this spin precession model is very useful.

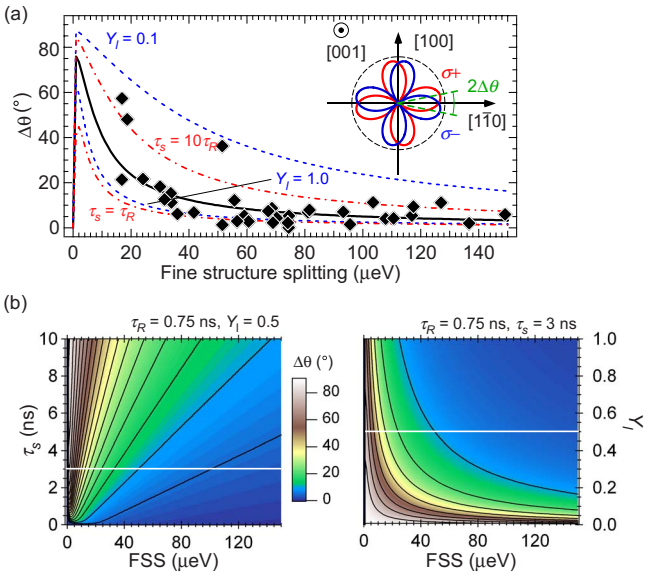

FIG. 3. (Color online) (a) δ_{b} dependence of $\Delta\theta$. Diamonds indicate the experimental data and curves indicate the calculated data. The solid curve is obtained at $\tau_{\mathrm{s}}=4\tau_{\mathrm{R}}$ ($T_{\mathrm{s}}=4\tau_{\mathrm{R}}/5$) and $Y_l=0.5$; dashed curves, at $\tau_{\mathrm{s}}=4\tau_{\mathrm{R}}$ and $Y_l=0.1$ and 1.0; dot-dashed curves, at $Y_l=0.5$ and $\tau_{\mathrm{s}}=\tau_{\mathrm{R}}$ and $10\tau_{\mathrm{R}}$ ($T_{\mathrm{s}}=\tau_{\mathrm{R}}/2$ and $10\tau_{\mathrm{R}}/11$). Inset: polar plots of calculated PL polarization for σ_+ and σ_- polarized excitations. Depending on the sign of P_c, the polarization axis varies to $2\Delta\theta$. (b) 2D plot of $\Delta\theta$ as functions of δ_{b} and τ_{s} (left panel) and Y_l (right panel). The solid horizontal lines in each panel correspond to the solid curve of (a).

Let us consider the phase difference of the DLP depending on the excitation orientation. The initial spin vectors created by circularly polarized photons (σ_+, σ_-) point toward the poles of the Bloch sphere. Although each vector starts precessing around $\boldsymbol{\Omega}$, the axes of the observed DLP are symmetrical for $[1\bar{1}0]$, because both $\boldsymbol{\Omega}$ and $\boldsymbol{P}_{\mathrm{eq}}$ are directed toward $[1\bar{1}0]$ according to our assumption. If the deviation of the DLP axis from $[1\bar{1}0]$ is denoted by $\Delta\theta$, angle difference obtained from the σ_+ and σ_- excited DLP curves [Fig. 3(a) inset] is given by $2\Delta\theta$. Astakhov *et al.*[4] observed a large angle difference of $2\Delta\theta=67°$ in CdSe/ZnSe QD ensemble which consists of 10^8 QDs. Comparing with $\Delta\theta$ and the calculation, they estimated Ω_{exc} and T_{s} as on the order of tens microelectron volts and of a hundred picoseconds, respectively. Although they successfully explained the polarization behavior with the similar precession model, detailed experiments concerning with the variation in Ω_{exc} have not been done yet. Observation of single QDs reveals the relation between Ω_{exc} and polarization conversion efficiency as well as polarization axis, therefore the rigorous investigation of the applied model can be performed.

We measured $\Delta\theta$ for a number of InAlAs QDs with different FSS and plotted it as a function of δ_{b} [Fig. 3(a)]. The left (right) side panel of Fig. 3(b) shows the calculated two-dimensional (2D) plot of $\Delta\theta$ as functions of δ_{b} and τ_{s} (Y_l). From the experimental and calculated results, it is found that

$\Delta\theta$ decreases with increasing δ_b. If a QD has a large δ_b, the spin vector precesses with a large angular frequency, and the steady-state value comes close to Y_l, regardless of the state of excitation polarization. As a result, $\Delta\theta$ reduces with increasing δ_b. Furthermore, it is found that a large τ_s and a small Y_l yield a large $\Delta\theta$. In the absence of Y_l, since the axis of the spin due to a σ_+ or σ_- photon precesses in the yz plane, the polarization axis with σ_+ (σ_-) excitation is oriented along [100] ([010]) or [010] ([100]). Therefore, $\Delta\theta$ does not depend on the precession frequency and is always 90°. In general, $\Delta\theta$ is determined by the balance between τ_s/τ_R and Y_l. As compared to the calculation curves, the spin-relaxation time of a neutral exciton, τ_s, and the polarization equilibrium Y_l can be estimated roughly by using the recombination lifetime $\tau_R=0.75$ ns, which is obtained independently by time-resolved streak measurements for a single InAlAs QD in the same sample. In Fig. 3(a), the solid curve is obtained at $\tau_s=4\tau_R$ ($T_s=4\tau_R/5\sim0.6$ ns) and $Y_l=0.5$; dashed lines, at $\tau_s=4\tau_R$ and $Y_l=0.1$ and 1.0; and dot-dashed lines, at $\tau_s=\tau_R$ and $10\tau_R$ ($T_s=\tau_R/2$ and $10\tau_R/11$) and $Y_l=0.5$. Since parameters such as Y_l, τ_s, and τ_R are different for individual QDs, a deviation from the calculated curves is observed. However, many QDs lie around the curve with $\tau_s\sim4\tau_R$ and $Y_l=0.5$, which are typical values for average $In_{0.75}Al_{0.25}As$ QDs. The obtained spin-relaxation time agrees well with our previous results evaluated by using the four-wave mixing technique for the same In/Al-ratio QD ensemble under a zero magnetic field ($\tau_s\sim5\tau_R$),[16] and using the photon correlation method for a single InAlAs QD ($\tau_s\sim3.6\tau_R$).[7]

Here, we shall consider the large DLP observed in Fig. 1(c). As we have seen, the polarization conversion can be described by the spin precession model, and the amplitude of DLP is written as $\sqrt{\rho_l^2+\rho_{l'}^2}$. However, this large DLP of ~20% cannot be explained only by the effect of VBM and the thermal relaxation. In fact, the expected amplitude of DLP is about 10% by using Eqs. (2) and (3) with the parameters $\tau_s=4\tau_R$ and $Y_l=0.5$. At the present stage, we consider the optically created nuclear field contributes to this large DLP. It is well known that continuous circular polarized excitation induces a nuclear magnetic field (B_N) that is parallel or antiparallel to the external magnetic field, and its direction is decided by the helicity of the excitation polarization.[17] If small B_N corresponding to the energy shift of ~5 μeV is created, the magnitude of DLP rises up to ~17% with the same parameters by using the same precession model under a longitudinal magnetic field expressed in Eqs. (5) and (6). This estimation strongly suggests the formation of B_N. This effect of B_N will be discussed again in the next section.

C. Under longitudinal magnetic field

In order to investigate the exciton spin dynamics in detail and to achieve more efficient polarization conversion, similar experiments (that is, C→L conversion) under a longitudinal magnetic field B_z were performed for a typical single QD. In the same way with the previous section, first we explain the experimental results by using a simple model not including the nuclear field, and subsequently investigate the effect of

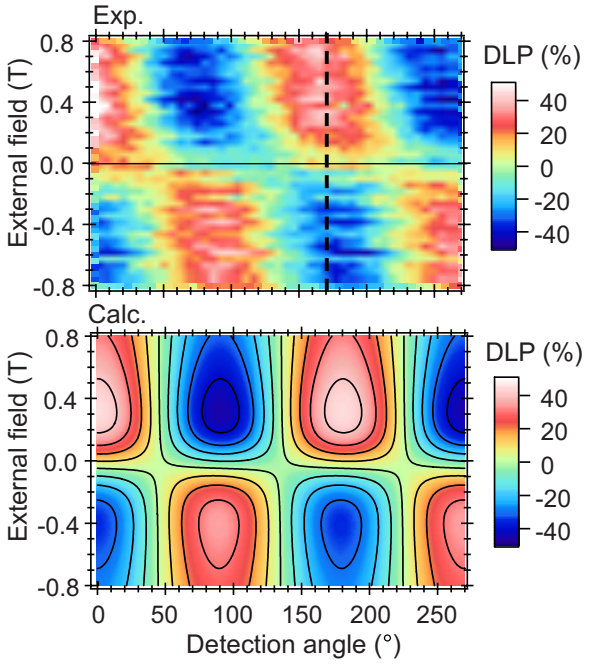

FIG. 4. (Color online) Contour plot of C→L conversion for target QD with $\delta_b=50$ μeV and $g_X=2.20$. DLP as functions of B_z and φ; experimental results (upper panel) and calculated results (lower panel). Other parameters used in the calculation are $\tau_R=0.75$ ns, $\tau_s=3$ ns, and $Y_l=0.5$.

the nuclear field. B_z modifies the torque vector as $\mathbf{\Omega}=(\Omega_{exc},0,\Omega_Z)$ and lifts it off the xy plane, as shown in Fig. 2(a). Ω_Z is the precession frequency due to the Zeeman splitting and is given by $g_X\mu_B B_z/\hbar$, where g_X is the exciton g factor in the growth direction and μ_B is the Bohr magneton. For this InAlAs QD, g_X is found to be 2.20 ± 0.01 by magneto-PL measurement under linearly polarized excitation. By using the above-mentioned precession model, the steady-state polarizations of the emission at the circularly polarized excitation $\boldsymbol{P}_{ex}=(0,0,P_c)$ are written as follows:

$$\rho_l=-\frac{\Omega_Z T_s \Omega T_s}{1+(\Omega T_s)^2}\left[\frac{T_s}{\tau_s}\frac{\Omega_Z}{\Omega}Y_l-\frac{T_s}{\tau_R}\frac{\Omega_{exc}}{\Omega}P_c\right]+\frac{T_s}{\tau_s}Y_l, \quad (5)$$

$$\rho_{l'}=+\frac{\Omega T_s}{1+(\Omega T_s)^2}\left[\frac{T_s}{\tau_s}\frac{\Omega_Z}{\Omega}Y_l-\frac{T_s}{\tau_R}\frac{\Omega_{exc}}{\Omega}P_c\right], \quad (6)$$

$$\rho_c=+\frac{\Omega_{exc} T_s \Omega T_s}{1+(\Omega T_s)^2}\left[\frac{T_s}{\tau_s}\frac{\Omega_Z}{\Omega}Y_l-\frac{T_s}{\tau_R}\frac{\Omega_{exc}}{\Omega}P_c\right]+\frac{T_s}{\tau_R}P_c. \quad (7)$$

Here, Ω is given as $|\mathbf{\Omega}|=\sqrt{\Omega_{exc}^2+\Omega_Z^2}$. If Y_l is zero and no spin decay takes place, the magnitude of DLP, $\sqrt{\rho_l^2+\rho_{l'}^2}$, reaches the maximum value of 50% at the external field $B_z=\delta_b/(g_X\mu_B)$. However, since Y_l is not zero in the InAlAs QD, as will be shown later, discussion about the maximum value of conversion efficiency will be more complicated. The upper panel of Fig. 4 shows the observed DLP as functions of B_z and φ. Not only the DLP amplitude but also its pattern are reproduced very well by the calculated DLP shown in the lower panel. In the calculation, the following parameters

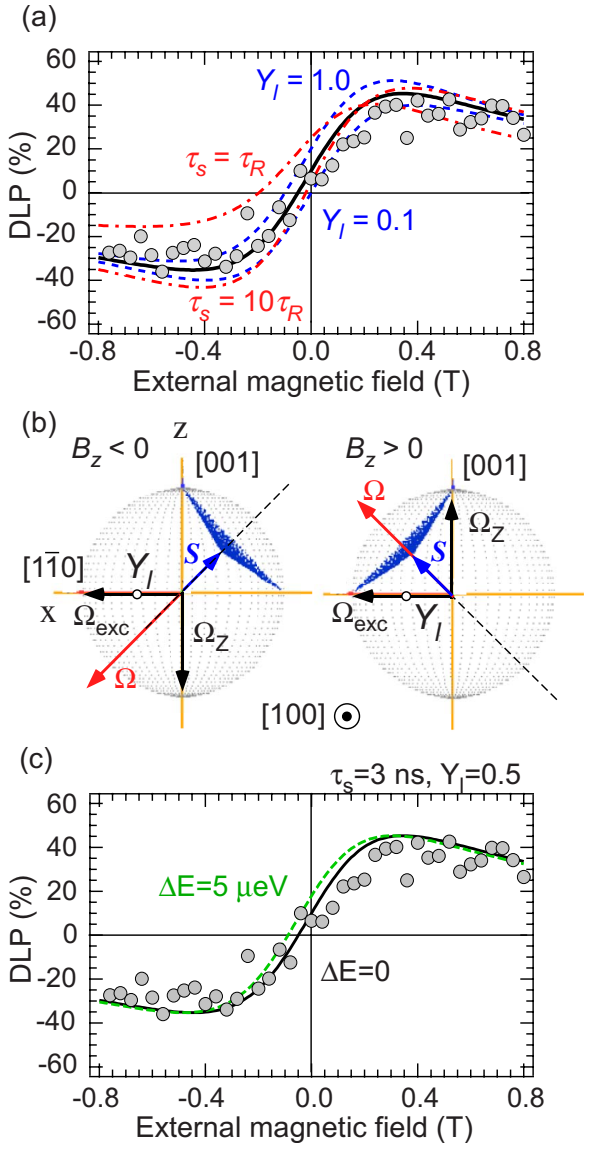

FIG. 5. (Color online) (a) Cross-section curve corresponding to the dashed line in Fig. 4. At the external field $B_z \sim \delta_b / g_X \mu_B$, the maximum value of DLP was observed. The solid curve is obtained at τ_s=3 ns and Y_l=0.5. For the dashed and dot-dashed curves, the calculation parameters are the same as those in Fig. 3(a). (b) Sketches of spin and torque vectors in the Bloch sphere under a longitudinal magnetic field $B_z<0$ (left) and $B_z>0$ (right). (c) B_z dependence of DLP including the effect of B_N. Compared with the solid curve (not including ΔE), the dashed curve (including ΔE of 5 μeV) is translated by ~40 mT down to the lower B_z values.

were used: τ_R=0.75 ns, τ_s=3 ns, and Y_l=0.5; further, the effect of the nuclear field was not included.

In Fig. 5, we show the DLP on the profile of the dashed line in the 2D plot shown in Fig. 4. At $|B_z| \sim 0.35$ T, the DLP shows a maximum (minimum) when B_z is positive (negative). The energy of the Zeeman splitting induced by this external field is the same as the energy of FSS (i.e., $\delta_b \sim g_X \mu_B B_z$), and the conversion efficiency reaches ~50%. Further, an increase in $|B_z|$ reduces the DLP amplitude, and this indicates that the polarization of the emitted light becomes closer to circular polarization. Since the longitudinal magnetic confinement corrects the potential asymmetry, the effect of AEI will diminish under a large magnetic field (approximately several teslas). In addition, the asymmetric feature of the DLP amplitude about the B_z=0 T line can be explained by the effect of the spin equilibrium Y_l. As shown by Eq. (1), the effect of spin relaxation characterized by τ_s depends on $\Delta \boldsymbol{S}$, which is the vector component of $(\boldsymbol{S}-\boldsymbol{P}_{eq})$. In short, a large $\Delta \boldsymbol{S}$ induces a significant spin decay due to spin relaxation, and therefore, results in the reduction in the DLP. In the case of $B_z>0$, as shown in Fig. 5(b) right panel, $\boldsymbol{\Omega}$ (or $\boldsymbol{S}$) and Y_l are in the same half sphere ($x \geq 0$). However in the case $B_z<0$, as shown in Fig. 5(b) left panel, since the direction of $\boldsymbol{\Omega}$ is opposite and $\boldsymbol{S}$ precesses in the half sphere ($x \leq 0$), $\Delta \boldsymbol{S}$ on the average is larger than that in the former case, resulting in the asymmetric feature of the DLP depending on the sign of B_z. Although the precise evaluation of the magnitude of Y_l is difficult, this fact implies that Y_l has a finite value; it is estimated as ~0.5 for the target QD. The result calculated by using Y_l=0.5 and τ_R=0.75 ns, is shown by the solid curve in Fig. 5(a), and τ_s is roughly estimated to be 3 ns. This is quite consistent with the estimated value of $\tau_s \sim 4\tau_R$ obtained under a zero magnetic field. Further, it is found that the DLP is not significantly sensitive to Y_l, although Y_l is one of the key quantities affecting it.

Then, we would like to consider the effect of the nuclear field under an external magnetic field. As mentioned in the previous section, a nuclear magnetic field B_N can be created with our experimental procedure. Actually, in other experiments on InAlAs QDs, we observed a large B_N corresponding to several teslas for an electron spin under a large external field ($B_z>3$ T) with wetting layer excitation.[17] If B_N is formed, Ω_Z changes to $\Omega_Z=(g_X \mu_B B_z+\Delta E)/\hbar$ and increases (decreases) under $B_z>0$ ($B_z<0$), because $\Delta E>0$ in the present excitation polarization. Here, ΔE is the Zeeman splitting induced by B_N (Overhauser shift) and is proportional to B_N. The dashed curve in Fig. 5(c) includes the effect of B_N as ΔE=5 μeV, where the other parameters used in the calculation are the same with the solid curves in Figs. 5(a) and 5(c) (that is, τ_s=3 ns and Y_l=0.5). Since the nuclear field works as an additional magnetic field, the DLP pattern shown in Fig. 4 and therefore the profiled curves shift to lower B_z values. Here it should be noted that the addition of B_N does not affect our findings not including the effect of B_N except for the change in DLP around 0 T. As shown in Fig. 5(c), ΔE of 5 μeV translates the DLP curve only by ~40 mT in this QD with g_X=2.20, and this change is not significant. The small B_N corresponding to $\Delta E \sim 5$ μeV is reasonable under the present experimental conditions (low $|B_z|<1$ T, quasiresonant excitation).[18] Though the experimental results under zero and nonzero external magnetic fields indicate B_N formation indirectly, at present we cannot detect B_N as Overhauser shift because the energy shift of 5 μeV is comparable to our spectral resolution. More quantitative discussion about the effect of B_N needs further experiments with higher spectral resolution.

Finally, let us stress again that the high DLP around a zero external magnetic field cannot be explained only by ordinary values of VBM in III-V QDs, and we found that even a small nuclear field affected polarization conversion significantly.

IV. SUMMARY

In summary, the polarization conversion from optical orientation to alignment in single InAlAs QDs was investigated under zero and nonzero magnetic fields. A lot of single QDs were investigated in terms of polarization conversion, and the results were explained consistently and closely by using a comprehensive model including a built-in linear dichroism. Quasiresonant excitation made it possible to inject highly polarized exciton spin, and consequently polarization conversion with a high efficiency of $\sim 50\%$ was achieved under a longitudinal magnetic field. Additionally, a large DLP under a zero magnetic field was well explained with the effect of the optically created nuclear field. Our results suggest strongly that even a small nuclear field brings a significant influence on the conversion efficiency under a zero magnetic field.

Y_l and τ_s/τ_R were estimated by measuring the angle difference of the DLP or the conversion efficiency. By using the recombination lifetime $\tau_R = 0.75$ ns, which was obtained by independent measurement, we evaluated τ_s and Y_l as ~ 3 ns and 0.5, respectively, for the target QD. The obtained τ_s was in a good agreement with our previous results obtained for the same In/Al-ratio QD ensemble under a zero magnetic field. This long spin-relaxation time, exceeding the recombination lifetime, gives valuable information regarding the spin-based applications such as quantum computations and single-photon sources.

ACKNOWLEDGMENTS

S.A. gratefully acknowledges the financial support of Support Center for Advanced Telecommunications Technology Research (SCAT). We are grateful for helpful conversations with H. Sasakura, H. Kumano, and Y. Toda concerning this work.

*r-kaji@eng.hokudai.ac.jp

[1] D. D. Awschalom, N. Samarth, and D. Loss, *Semiconductor Spintronics and Quantum Computation* (Springer, Berlin, 2002).
[2] M. Bayer, G. Ortner, O. Stern, A. Kuther, A. A. Gorbunov, A. Forchel, P. Hawrylak, S. Fafard, K. Hinzer, T. L. Reinecke, S. N. Walck, J. P. Reithmaier, F. Klopf, and F. Schäfer, Phys. Rev. B **65**, 195315 (2002).
[3] R. I. Dzhioev, B. P. Zakharchenya, E. L. Ivchenko, V. L. Korenev, Yu. G. Kusraev, N. N. Ledentsov, V. M. Ustinov, A. E. Zhukov, and A. F. Tsatsul'nikov, Phys. Solid State **40**, 790 (1998).
[4] G. V. Astakhov, T. Kiessling, A. V. Platonov, T. Slobodskyy, S. Mahapatra, W. Ossau, G. Schmidt, K. Brunner, and L. W. Molenkamp, Phys. Rev. Lett. **96**, 027402 (2006).
[5] H. Sasakura, S. Adachi, S. Muto, H. Song, T. Miyazawa, and T. Usuki, Jpn. J. Appl. Phys., Part 1 **43**, 2110 (2004).
[6] K. Kowalik, O. Krebs, A. Lemaitre, J. A. Gaj, and P. Voisin, Phys. Rev. B **77**, 161305(R) (2008).
[7] H. Kumano, S. Kimura, M. Endo, H. Sasakura, S. Adachi, S. Muto, and I. Suemune, J. Nanoelectron. Optoelectron. **1**, 39 (2006).
[8] S. Adachi, H. Sasakura, N. Yatsu, R. Kaji, and S. Muto, Appl. Phys. Lett. **91**, 161910 (2007).
[9] T. Tsuchiya, Physica E (Amsterdam) **7**, 470 (2000).
[10] E. L. Ivchenko, *Optical Spectroscopy of Semiconductor Nanostructures* (Alpha Science International, Harrow, UK, 2005).
[11] A. V. Koudinov, I. A. Akimov, Yu. G. Kusrayev, and F. Henneberger, Phys. Rev. B **70**, 241305(R) (2004).
[12] Y. Léger, L. Besombes, L. Maingault, and H. Mariette, Phys. Rev. B **76**, 045331 (2007).
[13] R. J. Epstein, D. T. Fuchs, W. V. Schoenfeld, P. M. Petroff, and D. D. Awschalom, Appl. Phys. Lett. **78**, 733 (2001).
[14] A. S. Bracker, E. A. Stinaff, D. Gammon, M. E. Ware, J. G. Tischler, A. Shabaev, Al. L. Efros, D. Park, D. Gershoni, V. L. Korenev, and I. A. Merkulov, Phys. Rev. Lett. **94**, 047402 (2005).
[15] Y. Masumoto, S. Oguchi, B. Pal, and M. Ikezawa, Phys. Rev. B **74**, 205332 (2006).
[16] T. Watanuki, S. Adachi, H. Sasakura, and S. Muto, Appl. Phys. Lett. **86**, 063114 (2005).
[17] R. Kaji, S. Adachi, H. Sasakura, and S. Muto, Appl. Phys. Lett. **91**, 261904 (2007).
[18] We confirmed experimentally that the formation of large B_N is suppressed under the quasiresonant excitation in InAlAs QDs. This can be explained by the reduction in the fraction time that an electron occupies the QD.